Proceedings of ASME Turbo Expo 2011
GT2011
June 6-10, 2011, Vancouver, British Columbia, Canada

GT2011-45784

IMPACT OF MISTUNING ON THE VIBRATION BEHAVIOUR OF THE LAST STAGE IN A MODEL THREE STAGE LOW PRESSURE STEAM TURBINE

Christoph Heinz*, Markus Schatz, Michael V. Casey

ITSM, Institute of Thermal Turbomachinery and Machinery Laboratory, Stuttgart, Germany

Heinrich Stüer

Siemens AG, Energy Sector, Fossil Power Generation, Steam Turbine Technology, Mülheim a. d. Ruhr, Germany

ABSTRACT

The last stages of a low-pressure steam turbine, with long freestanding blades, may experience forced response excitation during resonance crossing at start-up and shut-down and this can be responsible for blade failure.

This paper presents an experimental investigation of the circumferential blade amplitude distribution at different operating conditions and for different mistuning configurations in a scale model of a state-of-the-art low pressure steam turbine.

Five configurations are investigated; two with different intentionally mistuned frequency arrangements, where the blades are placed alternately in different high-low configurations and three randomly mistuned systems. For the randomly mistuned systems the standard deviation of the resonance frequencies of the last stage blades is varied. The maximum blade amplitude and the circumferential blade amplitude distribution of each mistuning configuration are compared at different operating points and at a repeatable rotational speed gradient.

The behaviour of the blade amplitude distribution at different operating conditions shows that the vibration levels depend on both the mistuning configuration and the operating points.

NOMENCLATURE

FRF	Frequency response function
MBVM	Tip timing system
$\dot{m}_{rel}$	Normalized mass flow rate
OP	Operating Point
p_c	Normalized condenser pressure

1 INTRODUCTION

In a modern electrical grid, the high variability of the demand for electricity requires that steam turbines can cope with a wide range of load variation. To guarantee a faultless operation during such flexible operation it is necessary to know the dynamic performance of the machine. In all turbomachines, but especially in the last stage blades of a low pressure steam turbine, forced response excitation during resonance crossing at start-up and shut-down can be responsible for blade failure as during these processes a wide range of different resonant frequencies are excited. In each of these resonance points the system responds to the aerodynamic loads with varying blade amplitudes. These amplitudes depend on blade damping and aerodynamic coupling as well as on different mistuning parameters.

The mistuning parameters and the coupling through the rotor cause the vibration amplitude to vary strongly from blade to blade. This paper presents an experimental investigation of the circumferential blade amplitude distribution at different operating conditions and different mistuning configurations. A summary of experimental approaches concerning this high cycle fatigue (HCF) phenomenon was previously presented by Srinivasan [1].

The high variation of blade amplitudes during resonance crossing is based on small differences in blade resonance frequencies as well as on the variation of blade damping parameters. The frequency differences are caused by manufacturing tolerances or intentional mistuning while the damping variations are effected by small differences in the blade attachment at the blade root or different aerodynamic conditions. The increase of blade stresses in just a few blades of a blade row can lead to premature fatigue. This variation of blade amplitudes and its

* corresponding author

generating factors have been investigated in many publications in the past.

Wagner [2] has shown analytically and experimentally that the coupling through the rotor is a very important factor with regard to the blade amplitude distribution in a blade row. Wei and Pierre [3] showed that the sensitivity of blade amplitude distribution on mistuning depends primarily on the ratio of mistuning strength to coupling strength.

Whitehead presented analytical work [4, 5] in which he has derived that for a certain symmetric distribution of the mistuned blades the maximum amplification factor for an individual engine order compared to a tuned system with equally damped blades is

$$\frac{1}{2}\cdot(1+\sqrt{N}) \tag{1}$$

where N is the number of blades in a row. Another approach in order to determine the worst mistuning patterns in bladed disks was published by Petrov and Ewins [6] in 2003. It is based on FE calculations and uses an optimization approach.

In the following years, many authors [7-10] published theoretical studies dealing with the question of how to reduce the blade amplification compared to a tuned system, where all blades are identical. Feiner and Griffin developed the “Fundamental Mistuning Model” (FMM), a simplified method which allows the vibration amplitudes to be calculated for individual mode families with comparably low effort [11]. This method was developed further, so that it is possible to calculate the mistuning parameters from the measured blade amplitudes without having to determine the natural frequencies [12]. This method was validated experimentally on a two stage compressor [13].

Heinz et al. [14] showed the behaviour of an intentionally mistuned system at different operating conditions. By fitting the experimental data with an indirect correction procedure, blade amplitudes could be predicted well for a part of the turbine characteristic.

The objective of this paper is to determine the influence of different mistuning configurations on both the circumferential blade amplitude distribution and on the maximum blade amplitude in the last stage at the resonance crossing of first bending mode and second engine order F1/EO2. The behaviour of the blade with the maximum amplitude is studied for different operating conditions. It can be shown that with systematic mistuning the amplitude of the blade with the highest stress level can be strongly reduced. Five different mistuned systems are investigated, see tables 2 and 3. Two of them have an alternating high-low arrangement of the blade resonance frequencies with varying difference between high and low tuned blades (configuration B.1 and B.2). Configuration A.1 – A.3 are randomly mistuned systems, whereby A.1 and A.2 have the same standard deviation of blade frequencies but different individual blade frequencies and A.3 exhibits a reduced standard deviation.

2 MODEL TURBINE

In this section, a quick overview of the test rig is given in which the experiments have been done and the measurement equipment is explained. A more detailed description of the steam turbine test rig can be found in [15].

2.1 Test stand

The test rig is a steam-driven three stage turbine, modeling the final stages of power plant low pressure steam turbines, scaled with a factor of 4.2. Figure 1 shows a cross section of the whole test stand. The power output is dissipated using a water brake. At the low pressure end, there is an auxiliary turbine. This turbine is used for investigating the windage operation, where the mass flow through the machine is not sufficient to maintain nominal speed as the last stage rotor actually conveys shaft power to the working fluid.

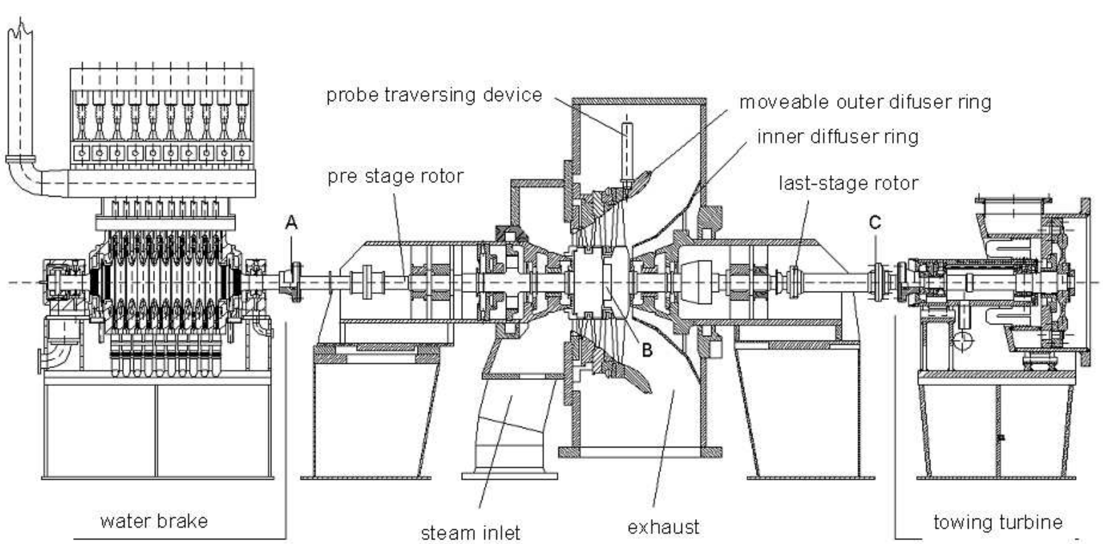

Figure 1: Test stand for LP model steam turbine at ITSM

In the present study, the vibration behaviour of the last stage of the model steam turbine is analyzed. For the investigations during the start-up process, the water brake is used to adjust different mass flow rates.

By varying the relative condenser pressure p_c between 0.25 and 1, the influence of the aerodynamic condition on the vibration behaviour can be shown. For the present publication, the pressure has been normalized with the maximum condenser pressure used in the course of the investigation. To guarantee a predefined and repeatable sweep with different rotor speed gradients through the resonance area, an automatic sweep controller was implemented into the test stand control system.

2.2 Measurement Equipment

In order to capture the blade frequencies and amplitudes, two different measurement systems are used. Figure 2 shows 12 blades (green colored) which are instrumented with strain gauges. However, to determine the circumferential amplitude distribution, the vibration data of all blades are necessary.

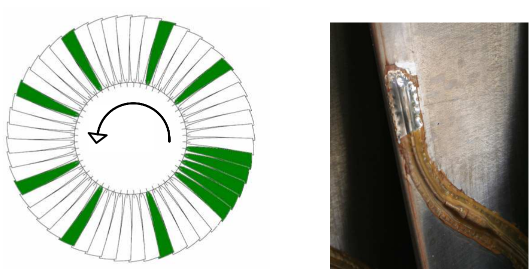

Figure 2: Blades instrumented with strain gauges

Therefore a new tip timing system developed by Siemens AG is used for the identification of the vibration behaviour of all blades. This system works with 8 equally spaced inductive sensors, shown in Fig. 3. Therefore an undersampling of the resonance area can be avoided . The vibration analysis is done with an in-house Siemens algorithm. The validation of the tip timing system is performed with strain gauge data.

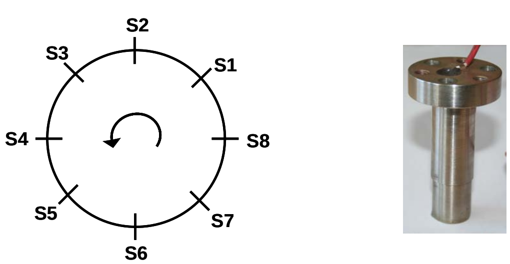

Figure 3: Sensor arrangement tip timing system

3 EXPERIMENTAL APPROACH

The objective of this work is to characterize the vibration behaviour of a last stage steam turbine during resonance. The investigation was carried out at six operating points (OP 1 to OP 6), which are shown in table 1. The mass flow rate is defined at the beginning of the sweep, during which the rotational speed is increased by 1000 rpm through the resonance area with a gradient of 4 revolutions per second. The mass flow is normalized with the maximum mass flow investigated, and the pressure with the maximum condenser pressure used during the experiments.

Table 1: Operating points (OP)

OP	$\dot{m}_{rel.}$[ ]	p_c[ ]
1	**0.61**	**0.25**
2	**0.67**	**0.3**
3	**0.89**	**0.3**
4	**1**	**0.3**
5	**0.95**	**0.5**
6	**0.95**	**1**

3.1 Amplitude determination

Since two measurement systems are used to measure the blade amplitudes at a resonance frequency, two different analysis methods are applied. To determine the amplitude of the blade from strain gauge measurement data, firstly the excited resonance frequency is identified using a Fast Fourier Transformation (FFT).

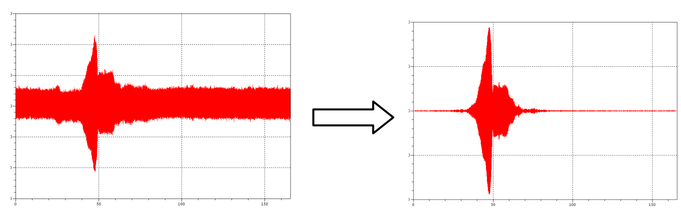

Figure 4: Raw and filtered time signal around resonance frequency

In order to extract the amplitude of the blade vibration at this frequency, the time signal is filtered by an FIR band-pass filter in a range of +/- 5 Hz around the resonance frequency (see Fig. 4). The strain value obtained is multiplied by a factor determined from FEM simulations of the blade to calculate the blade amplitude.

With the tip timing system, the signals of the eight sensors are post-processed by Siemens internal software. With this algorithm, the blade amplitude which is based on the tip deflection of the blade and the respective excited resonance frequencies can be determined as well as the transfer function of the blade. Afterwards, the comparison of results obtained from TTM and strain gauge measurements can be performed. The blade amplitudes and frequencies given in this publication are normalized using the average resonance frequency and the blade amplitude of a tuned system.

3.2 Frequency arrangement

Five mistuning configurations have been investigated in this paper. For configuration A.1, A.2 and A.3, the blades are arranged randomly (see Fig. 5-6). Their specific mistuning values are given in table 2. All frequency distributions shown in this section are measured at an identical operating point.

Table 2:: Specific mistuning values for configuration A

Configuration	A.1	A.2	A.3
Average frequency [ ]	1.034	1.032	1.03
Standard deviation $\sigma_{rel.}$ [%]	0.58	0.59	0.33

For A.1 and A.2 the standard deviations have nearly identical values. The difference between A.1 and A.2 can be shown in Fig. 5, where for A.2 blade 2, 3, 11, 18, 19, 48 and 49 are treated in order to reduce their resonance frequencies. In addition, the average frequency is a little lower. All other blades have nearly identical resonance frequencies, although a very small increase of the frequencies of all blades is visible. This can be explained by measurement uncertainties, which are less than 0.5%.

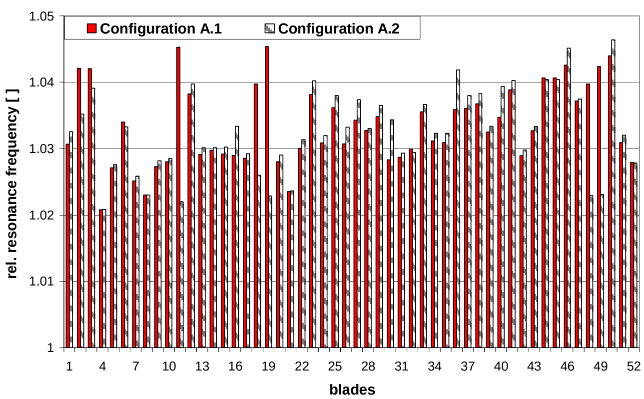

Figure 5: Relative frequency arrangement of configuration A.1 and A.2

Figure 6 shows configuration A.1, but now in comparison with configuration A.3. Configuration A.3 has a more uniform frequency distribution which results in strongly reduced standard deviation. This configuration again has a slightly reduced average resonance frequency, but these average values are not relevant for the interpretation of the quality of the different arrangements.

Table 3: Specific mistuning values for configuration B

Configuration	B.1	B.2
Avg. high tuned frequency [ ]	1.02	1.02
Avg. low tuned frequency [ ]	1.005	0.985
$\Delta_{high-low}$ [ ]	0.015	0.035

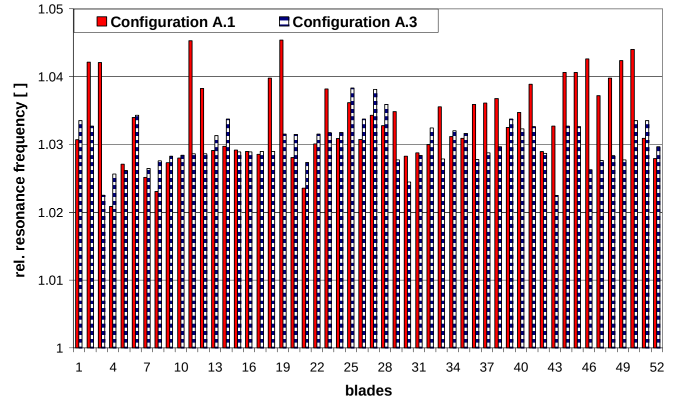

Figure 6: Rel. frequency arrangement of configuration A.1 and A.3

In contrast to the randomly mistuned arrangements A.1 - A.3, configuration B includes two different intentionally mistuned frequency distributions, B.1 and B.2. Both have an alternating high - low arrangement in the first bending mode. Table 3 shows the specific values of these configurations.

While the high tuned frequencies remain unchanged, the difference between the average high tuned and average low tuned blades is more than twice as big for B.2 than for B.1. These two arrangements are visible in Fig. 7. On top if this, there is a small random deviation of the resonance frequencies in the low tuned blades as well as in the high tuned ones. This superposition of random and intentional mistuning causes an overlap between high and low tuned blades in configuration B.1.

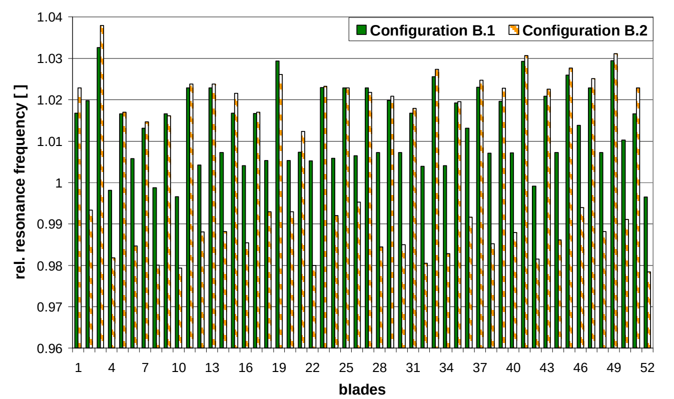

Figure 7: Frequency arrangement of configuration B.1 and B.2

In configuration B.2, the difference between both blade groups is large enough to avoid the overlap and two clearly separated blade groups exist, which are arranged in an alternating high – low assembly.

4 VALIDATION OF TIP TIMING DATA

The achievement of meaningful results is the major task of the validation of the tip timing system by means of strain gauges. In the next few figures the validation of resonance frequency, blade amplitudes and the frequency response function (FRF) is carried out with configuration B.1 at OP 5. Fig. 8 shows that the relative resonance frequencies measured with tip timing and strain gauges are in very good agreement. Small variations are caused by the resolution and the block length of the Fast Fourier Transformation (FFT).

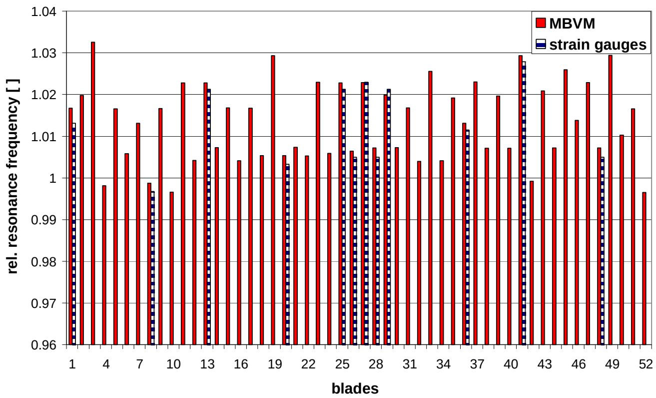

Figure 8: Validation of resonance frequencies at OP 5

Figure 9 shows the circumferential blade amplitude distribution and the comparison of the tip timing system and strain gauges for twelve blades. Again, a good agreement can be found. Some differences between both measurement systems can be detected, but the distribution of the measured strain gauge amplitudes can be reproduced well in the tip-timing system.

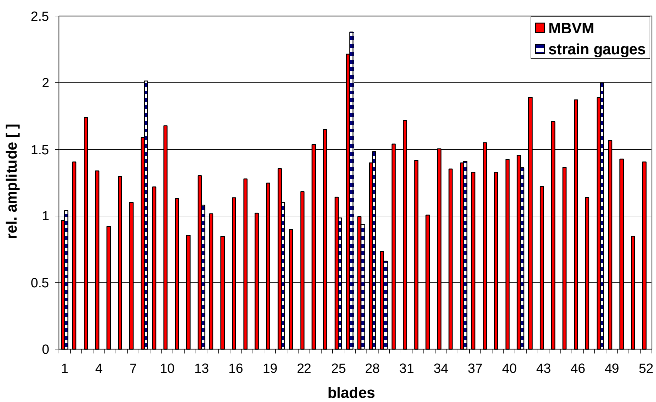

Figure 9: Validation of blade amplitudes at OP 5

In addition to amplitudes and frequencies, the frequency response function (FRF) also has to be validated. The FRF shows the behaviour of the system during the sweep across the resonance area. It is obtained by transforming the data along the second engine order from the time domain into the frequency domain by using an FFT. The sampling rate was 16384 Hz and the block length was chosen to be of 8192 samples, resulting in a frequency resolution of 0.5 Hz. Figure 10 shows the FRF of a blade responding with high amplitude. In this FRF only one peak is visible. This peak is found by the MBVM tip-timing system as well as with strain gauge data. Only the frequency belonging to the peak amplitude is shifted somewhat towards lower frequencies.

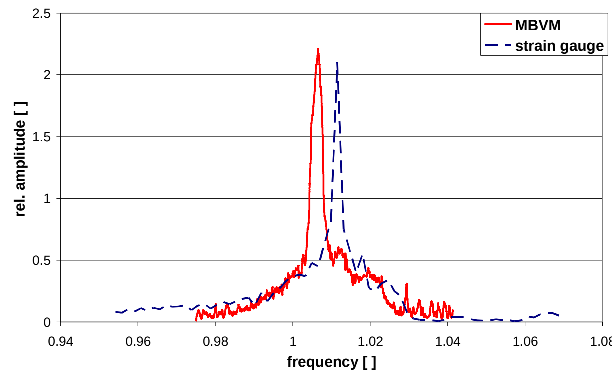

Figure 10: Validation of FRF at OP 5

Figure 11 shows the FRF of a blade responding with very low amplitude. Here multiple peaks are visible. Again, this distribution is represented by strain gauge measurement as well as by the tip timing system.

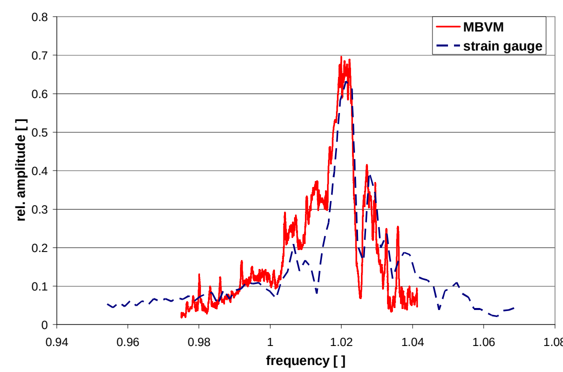

Figure 11: Validation of FRF at OP 5

5 RESULTS

In order to get an insight into the vibration behaviour of a mistuned last stage turbine, this section compares the different configurations against each other with regard to the maximum amplitudes. Moreover, the behaviour of configuration B.2 at different operating points is shown and the change of the amplitude distribution caused by a variation of the operating conditions is pointed out for different mistuning configurations. All frequency arrangements are investigated at two different operating points.

5.1 Amplitude distribution of configuration B.2

The vibration behavior of a lightly coupled system with freestanding blades is shown with the help of test case B.2 at different operating conditions. Firstly, Figure 12 shows the circumferential amplitude distribution and the amplification factor of each blade referring to OP2 at constant condenser pressure and different mass flow rates.

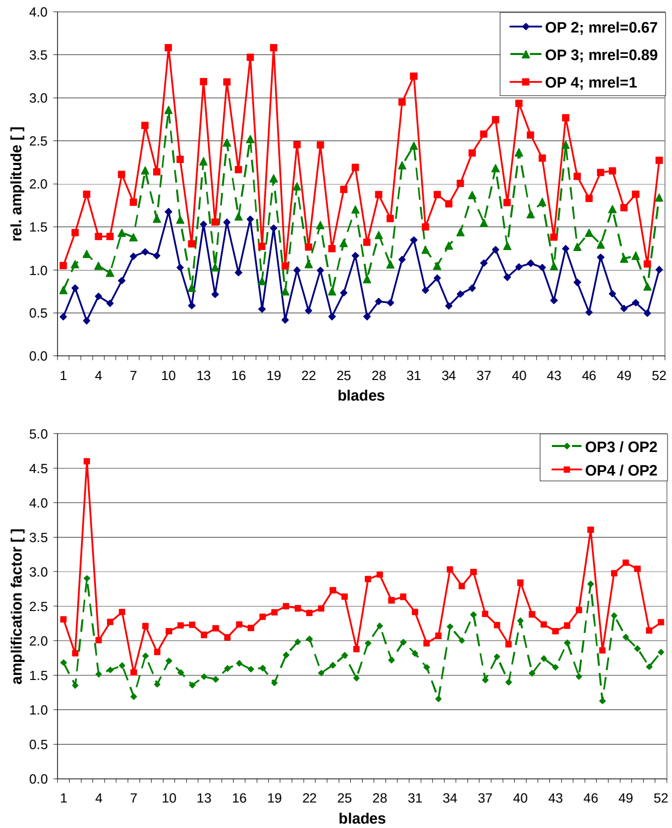

Figure 12: Different mass flow rates at constant condenser pressure p_c=0.3

It is evident that only the level of the amplitudes changes, but not the circumferential blade amplitude distribution. Interpreting the upper diagram with help of the amplification factors, it can be assumed that only the exciting forces increase with rising mass flow. The coupling through the aerodynamics seems to be almost unaffected. Fig. 13 shows the amplitude distribution for different condenser pressures at constant mass flow rate. In contrast to Fig. 12, where the amplitude distribution remains almost unchanged, the distribution is altered. Knowing that the variation of amplitude distribution depends primarily on the change of coupling conditions, the aerodynamic coupling has to be a function of the condenser pressure or the fluid density, respectively.

Another interesting question is whether the change in amplitude distribution due to varying operating conditions is only dependent on the change in condenser pressure (respectively fluid density) or also dependent on the mistuning configuration.

The changing circumferential amplitude distribution clearly shows the influence of coupling conditions on the blade vibration behaviour, which also affects the maximum blade amplitude of different mistuning configurations at different operating points.

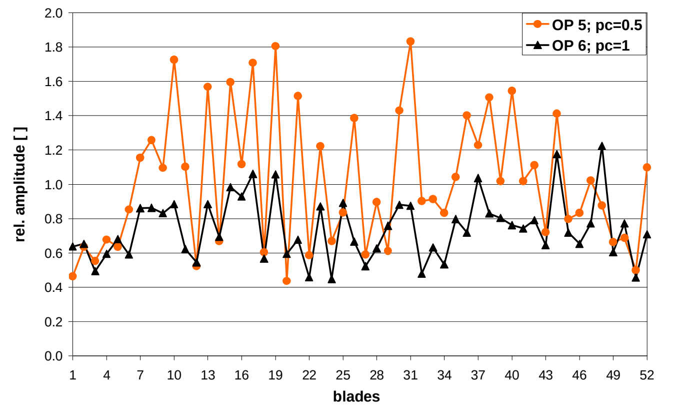

Figure 13: Different condenser pressures at constant mass flow rate $\dot{m}_{rel.}$= 0.95

This will be discussed in the next section, where different mistuning configurations are compared against each other with regards to the maximum amplitude as well as for the change in amplitude distribution due to varying operating conditions.

5.2 Comparison of different mistuning configurations

5.2.1 Amplitude distribution at OP 5

The most important indicator concerning the quality of the mistuning configuration is the blade with the maximum amplitude. This amplitude is decisive for blade failure. The next figures show a comparison of the maximum amplitudes of all configurations investigated. In figure 14, the amplitude distribution for test case A.1 and A.2, which have almost the same standard deviation, is given. Regarding configuration A.1, blade 10 has much higher amplitude than all other blades. This blade is responsible for the mechanical limit of the operating area of a steam turbine. Comparing this test case to A.2, it can be shown that the blade possessing the maximum amplitude changes to blade 19. As described in Fig.5, blade 19 is one of the blades whose natural frequency has reduced compared to configuration A.1. Thus it can be seen that even though the standard deviation stays almost unchanged, both the blade having the maximum amplitude as well as the level of the maximum amplitude changes. Although standard deviation is very similar, a difference in maximum blade amplitude of about 15% can be found.

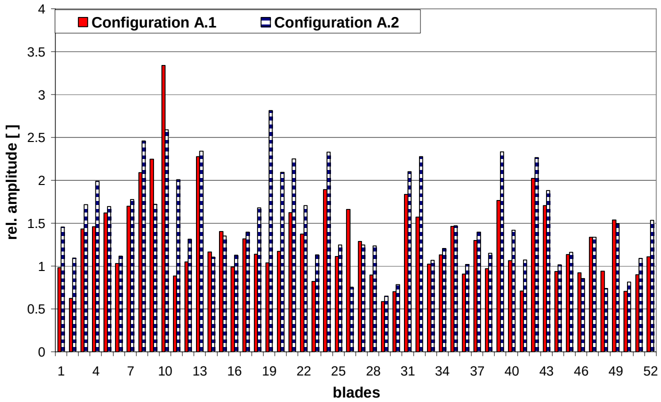

Figure 14: Amplitude distribution of Configuration A.1 and A.2

The effect of a reduction of the standard deviation was often presented in publications, but mostly calculated by means of analytical or numerical models. Fig.15 shows the change in circumferential amplitude distribution and for the maximum amplitude, when reducing the standard deviation from 0.59% to 0.33%. Regarding both distributions, A.3 has lower maximum amplitude (blade 4) compared to A.1, but almost the same maximum amplitude as test case A.2 (see Fig. 14). The circumferential amplitude distribution is completely different for both arrangements. As expected from available literature with theoretical investigations, the experimental results show that the maximum blade amplitude is not necessarily reduced when the standard deviation decreases.

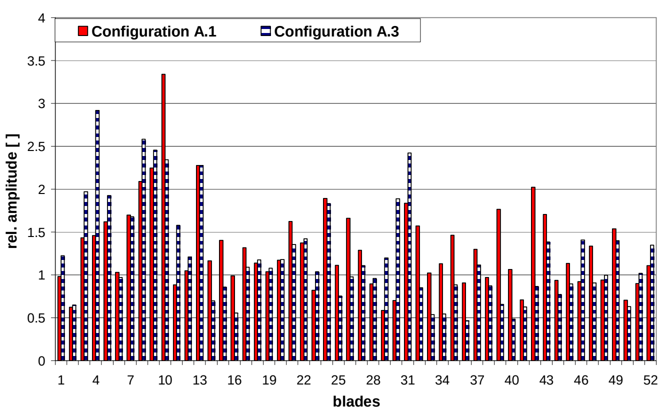

Figure 15: Amplitude distribution of Configuration A.1 and A.3

Besides these randomly distributed configurations, test case B.1 and B.2, are intentionally mistuned systems with a high-low arrangement of the blade resonance frequencies. Their amplitude distributions are shown in Fig. 16. Compared to Fig. 14 and 15, the maximum amplitude of both systems is much lower than those of configurations A.1-A.3. The comparison of B.1 and B.2 shows two different amplitude distributions and lower maximum amplitude for the configuration B.2, which is the one with the higher frequency difference between high and low tuned blades. Probably, based on the additional random mistuning which causes an overlap between high and low tuned blades for B.1, the amplitudes can be reduced by decoupling the neighbored blades with a specific frequency difference.

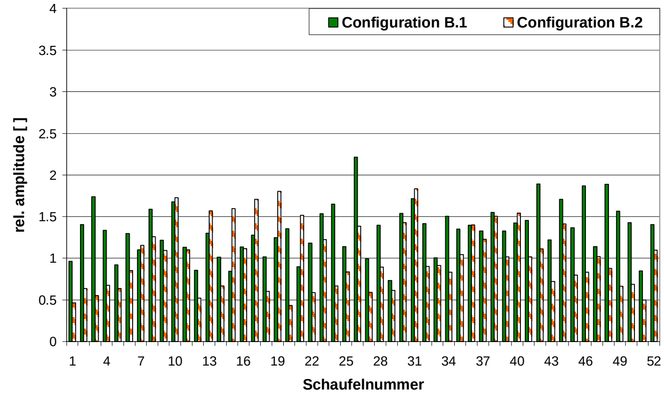

Figure 16: Amplitude distribution of Configuration B.1 and B.2

5.2.2 Maximum blade amplitudes

The maximum amplitude of each configuration previously shown before is given in Fig. 17, where the blades having the maximum amplitudes are compared against each other. Starting at A.1, an amplitude reduction at the alternating high - low arrangement of the blades of test case B can be shown. Higher difference between high and low tuned frequencies brings an additional reduction of blade amplitudes. When the maximum blade amplitudes at two different operating points are compared against each other, a small change in the characteristic is visible. Indeed, the trend is the same, configuration A shows a different behaviour at OP 1 than at OP 5 and seems to be much more sensitive to changes of the operating conditions than configuration B, where B.2 is always the one with the lowest maximum amplitude.

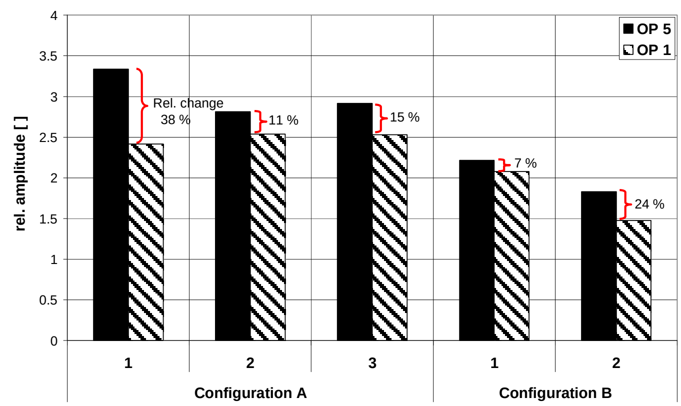

Figure 17: Maximum blade amplitudes compared at different OP

This behaviour and the change of the blade having the maximum amplitude due to the change of operating conditions are investigated in the next section.

5.2.3 Change of the circumferential blade amplitude distribution at different OP

In this section, the difficulty in predicting blade amplitudes of slightly coupled systems becomes evident. As already shown in Fig. 13, the amplitude distribution changes when the condenser pressure varies. An important question is how this change in amplitude distribution varies with the mistuning configuration. It is important to know whether the behaviour of the maximum blade amplitude changes or not for different mistuning configurations and different operating points. Figure 18 shows the amplitude distribution for configuration A.1 at OP1 and OP5. As visible, the blade experiencing the maximum amplitude as well as the blade amplitude distribution does not change. Regarding Fig. 19, where the same comparison is pointed out for the mistuning configuration A.3, it can be shown that the location of the blade subjected to the maximum amplitude is shifted from blade 10 (OP1) to blade 4 (OP5).

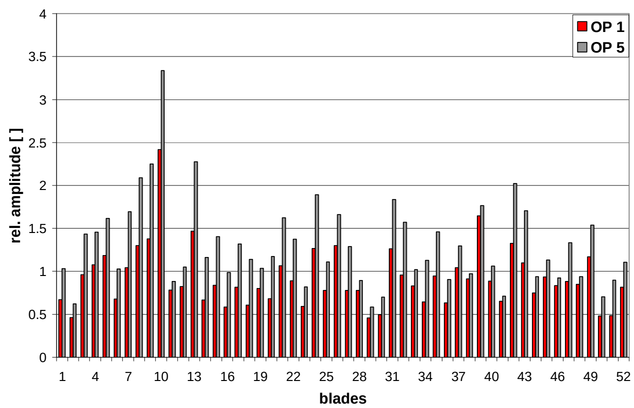

Figure 18: Comparison of the amplitude distribution at OP 1 and OP 5 measured with configuration A.1

This change of blade which exhibits the maximum amplitude constitutes a problem for the prediction of blade amplitudes in the case of forced response excitation, since not only the exciting force is changing, but also the aerodynamic coupling. As the aerodynamic coupling and damping of slightly coupled systems is hardly modeled in any theoretical approach for the prediction of the forced response behaviour, these experimentally observed phenomena are very difficult to be reproduced theoretically and hence can not be predicted very precisely.

In order to assess the extent of this problem and the influence of aerodynamic coupling and damping for different mistuning configurations, it is necessary to find a way of reflecting the strong dependency of the amplitude distribution on the mistuning configuration and operating conditions. To show the influence of mistuning, the variation of blade amplitude for all configurations (s. Figs.20-21) is compared when changing from OP 1 to OP 5.

$$\text{rel.change} = \frac{\text{rel. amplitude OP 5} - \text{rel. amplitude OP 1}}{\text{rel. amplitude OP 5}} \qquad (2)$$

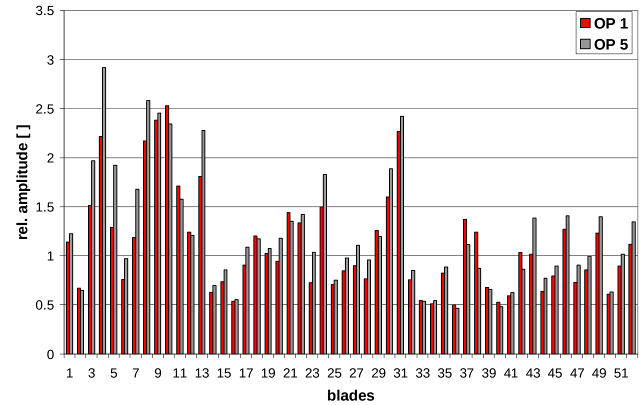

Figure 19: Comparison of the amplitude distribution at OP 1 and OP 5 measured with configuration A.3

For this purpose, the relative amplitude difference is used. This is the blade amplitude of OP 1 subtracted from the blade amplitude of OP 5 and divided by the blade amplitude of OP 5. (see eq. 2)

Regarding Fig. 20, where all randomly mistuned systems are shown, large differences in the relative amplitude change are visible. While test case A.1 shows a positive amplitude rise from OP 1 to OP 5, which is visible in a fairly consistent amplitude change for all blades, both other configurations exhibit a complete change of the blade amplitude distribution.

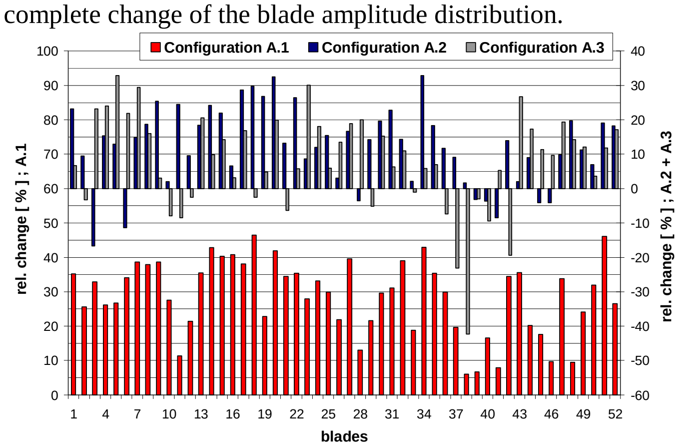

Figure 20: Relative change of each blade amplitude from OP 1 to OP 5 at different mistuning configurations

Regarding Fig. 21, where the amplitude change from OP 1 to OP 5 is shown for configuration B, it is again visible, that the amplitude change from OP 1 to OP 5 is as well arbitrarily as for configuration A. This means that the alternating mistuning arrangement has no stabilizing effect concerning the blade amplitude change due to the variation of the operating conditions.

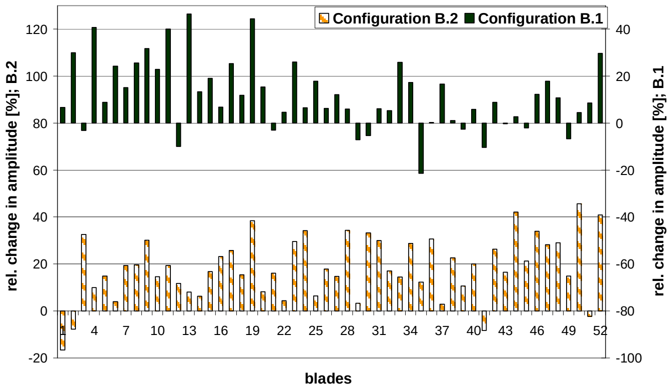

Figure 21: Relative change of each blade amplitude from OP 1 to OP 5 at mistuning configurations B.1 and B.2

Summarizing the analysis of this chapter, it can be pointed out that the intentionally mistuned systems show reduced maximum amplitudes, but with respect to the influence of the aerodynamic coupling, it can be assumed that there is an individual change in the blade amplitude distribution for changing operating conditions for the randomly mistuned system as well as for the intentionally mistuned system.

CONCLUSIONS

The vibration behaviour of a last stage model steam turbine during forced response excitation has been investigated experimentally. First of all a new tip timing system has been validated by means of strain gauge measurements. Both methods show very good agreement for the resonance frequency as well as for the blade amplitudes and the FRF. Following this, five different mistuning configurations have been investigated. Three of them (A.1-A.3) are randomly mistuned, in which A.1 and A.2 exhibit almost identical standard deviations. A.3 has more equally tuned blades with a reduction of the standard deviation of about 44%. Test case B.1 and B.2 are intentionally mistuned with a high – low arrangement of the blade eigenfrequencies. Test case B.1 has a frequency difference between high and low tuned blades which is half as large as the difference at configuration B.2. Due to the additional random mistuning at B.1 and B.2 there is an overlap of high and low tuned frequencies at B.1. The main results are:

- An amplitude reduction by implementing the high-low mistuning arrangement can be shown. The arrangement with the larger frequency difference, resulting in no frequency overlap of the neighboring blades (B.2) shows the lowest maximum blade amplitude. The reduction of the maximum amplitude is 45% in reference to A.1 at OP 5.
- The circumferential amplitude distribution depends strongly on the condenser pressure, whereas the mass flow rate has only influence on the amplitude level of the blades but not on the amplitude distribution itself.
- The impact of changing aerodynamic conditions and on blade amplitudes is depending on the mistuning configuration. It was found out that each mistuning arrangement has its own stability, respectively behaviour concerning its amplitude change caused by different operating conditions.

With this work it has been shown that the mistuning configuration not only influences the maximum blade amplitudes but also the behaviour of the system at varying operating conditions. Therefore, these results can be used in a first step for the validation of new analytical and numerical methods in order to find optimized blade arrangements which combine low maximum blade amplitudes and a stable behaviour for different operating conditions.

ACKNOWLEDGMENTS

The support of Siemens Energy and the permission to publish this work is kindly acknowledged. Part of the work presented in this paper was funded by “AG-Turbo, Verbundvorhaben COORETEC-turbo II; Teilvorhaben 4.3.2, FK 0327716K”. The responsibility for the content of the publication rests with the authors.

REFERENCES

[1] Srinivasan, A. V., 1997. “Flutter and Resonant Vibration Characteristics of Engine Blades”. *Journal of Turbomachinery*, **119**(4), pp. 741–775.
[2] Wagner, J. T., 1967. “Coupling of Turbomachine Blade Vibrations through the Rotor”. *Journal of Engineering for Power*, **89**, pp. 502–512.
[3] Wei, S. T., Pierre, C., 1988. “Localization Phenomena in Mistuned Assemblies with Cyclic Symmetry”. *Journal of vibration and acoustics*, **110**(4), pp. 429–449.
[4] Whitehead, D.S., 1966. “Effect of Mistuning on the vibration of Turbomachine Blades induced by wakes”. *Journal of Mechanical Engineering Science*, **8**, pp.15–21.
[5] Whitehead, D.S., 1998. “The Maximum Factor by Which Forced Vibration of Blades can increase due to Mistuning”. *Journal of Engineering for Gas Turbines and Power*, **120**(1), pp. 115–119
[6] Petrov, E.P., Ewins, D.J., 2003. ”Analysis of the Worst Mistuning Patterns in Bladed Disk Assemblies”. *Journal of Turbomachinery*, **125**(4), pp. 623-631
[7] Castanier, M.P., Pierre, C., 2002. “Using Intentional Mistuning in the Design of Turbomachinery Rotors”. *AIAA Journal*, . **40**(10), pp. 2077–2086
[8] Choi, B.-K., Lentz, J., Rivas-Guerra, A.J., Mignolet, M.P., 2003. “Optimization of Intentional Mistuning Patterns for the Reduction of the Forced Response Effects of Unintentional Mistuning: Formulation and Assessment”. Journal of Engineering for Gas Turbines and Power, **125**(1), pp. 131–140

[9] Hou, J, Cross, C., 2005. “Minimizing Blade Dynamic Response in a Bladed Disk through Design Optimization”. *AIAA Journal*, **43**(2), pp. 406–412
[10] Han, Y., Mignolet M. P., 2008. “Optimization of intentional Mistuning patterns for the Mitigation of the Effects of random Mistuning”. In ASME Turbo Expo 2008: Power for Land, Sea and Air, Berlin, ASME Paper GT-2008-51439
[11] Feiner, D.M., Griffin, J.H, 2002. “A Fundamental Model of Mistuning for a Single Family of Modes”. *Journal of Turbomachinery*, **124**(4), pp. 597–605
[12] Feiner, D.M.; Griffin, J.H, 2004. “Mistuning Identification of Bladed Disks Using a Fundamental Mistuning Model – Part I: Theory”. *Journal of Turbomachinery*, **126**(1), pp. 150–158
[13] Feiner, D.M., Griffin, J.H, 2004. “Mistuning Identification of Bladed Disks Using a Fundamental Mistuning Model – Part II: Application”. *Journal of Turbomachinery*, **126**(1), pp. 159–165.
[14] Heinz, Ch., Schatz, M., Casey, M.V., Stueer., H., 2010. “Experimental and analytical investigations of a low pressure model turbine during forced response excitation“. In ASME Turbo Expo 2010: Power for Land, Sea and Air, Glasgow, ASME Paper GT-2010-22146
[15] Wachter, J., Eyb, G., 1986. “Determination of the flow field in LP steam turbines”. In ASME Turbo Expo 1986, Düsseldorf, ASME Paper 86GT-210

